



Measurement of electron beam polarization from unstrained GaAs via two-photon photoemission

J.L. McCarter^{a,*}, A. Afanasev^b, T.J. Gay^c, J. Hansknecht^d, A. Kechiantz^{b,1}, M. Poelker^d

^a Department of Physics, University of Virginia, Charlottesville, VA 22901, USA

^b Department of Physics, The George Washington University, Washington, DC 20052, USA

^c Jorgensen Hall, University of Nebraska, Lincoln, NE 68588, USA

^d Thomas Jefferson National Accelerator Facility, 12050 Jefferson Avenue, Suite 500, Newport News, VA 23606, USA

ARTICLE INFO

Article history:

Received 19 September 2013

Received in revised form

24 October 2013

Accepted 15 November 2013

Available online 23 November 2013

Keywords:

Polarization

Two-photon

GaAs

Photocathode

Electron source

ABSTRACT

Two-photon absorption of 1560 nm light was used to generate polarized electron beams from unstrained GaAs photocathodes of varying thickness: 625 μm , 0.32 μm , and 0.18 μm . For each photocathode, the degree of spin polarization of the photoemitted beam was less than 50%, contradicting earlier predictions based on simple quantum mechanical selection rules for spherically-symmetric systems but consistent with the more sophisticated model of Bhat et al. (Phys. Rev. B 71 (2005) 035209). Polarization via two-photon absorption was the highest from the thinnest photocathode sample and comparable to that obtained via one-photon absorption (using 778 nm light), with values $40.3 \pm 1.0\%$ and $42.6 \pm 1.0\%$, respectively.

© 2013 Elsevier B.V. All rights reserved.

1. Introduction

Polarized electron sources are important components of particle accelerators, like the Continuous Electron Beam Accelerator Facility (CEBAF) at Jefferson Lab, where the spin of the electron beam is used to study nuclear structure, the dynamics of strong interactions, electro-weak nuclear physics, including parity-violation, and physics beyond the Standard Model [1]. The first GaAs-based polarized electron source used at an accelerator [2] provided beam polarization $\sim 35\%$, with a theoretical maximum polarization limited to 50% [3,4] due to the heavy-hole, light-hole energy level degeneracy of the $^2p_{3/2}$ valence band state (Fig. 1a). Significantly higher beam polarization was obtained in the 1990s by introducing an axial strain within the GaAs crystal structure [5–7] which eliminates this degeneracy (Fig. 1b). Today, beam polarization at accelerators routinely exceeds 80% using strained-superlattice GaAs/GaAsP structures [8,9]; however, these high-polarization photocathodes are thin compared to typical unstrained bulk GaAs and with respect to the photon absorption depth. As a result, strained-superlattice photocathodes exhibit significantly lower quantum efficiency (QE) than that of bulk GaAs samples [7,10].

Matsuyama et al. proposed using two-photon absorption, which is a non-linear optical process [11] that occurs only within crystals that lack inversion symmetry, as a mechanism to obtain high polarization from unstrained GaAs [12]. They reasoned that quantum mechanical selection rules associated with the simultaneous absorption of two photons of circularly-polarized light at half the band-gap energy would provide a means to populate the conduction band with electrons of just one spin state, yielding, in principle, completely polarized electrons in the conduction band immediately following excitation (Fig. 1c). According to this prediction, the electron polarization should be of opposite sign to that produced using single photon excitation. Subsequently, Matsuyama et al. [13] performed an experiment that relied on electron-hole photoluminescence measurements (but not photoemission) with electron-hole recombination fluorescence polarization measured to be 58%. This value was used to infer an electron polarization of 95% at the time of excitation to the conduction band [13]. While this result was consistent with an electron polarization of unity, the sign of the fluorescence polarization was inconsistent with their prediction.

In contrast to Ref. [13], a full examination of the quantum selection rules indicates that the transition depicted in Fig. 1c is not allowed, as two photons of like circular polarization must excite electron transitions with a change in azimuthal quantum number $\Delta\ell = 2$, which precludes a $^2p_{3/2}$ to $^2s_{1/2}$ transition at the Γ point. Bhat et al. [14] provided a detailed analysis of two-photon absorption in semiconductors, and predicted that polarization via two-photon absorption should be less than 50%. Photoluminescence

* Corresponding author. Present address: Laser and Plasma Technologies, 1100 Exploration Way, Hampton, VA 23666, USA. Tel.: +1 757 325 6783.

E-mail addresses: jlm2ar@virginia.edu, mccarter@jlab.org (J.L. McCarter).

¹ On leave from Institute of Radiophysics and Electronics, NAS of Armenia, Ashtarak 0203, Armenia.

experiments using differential transmission pump/probe techniques indicated a nascent polarization equal to 48%, in support of their predictions [14,15].

This paper presents the first direct measurement of electron beam polarization resulting from two-photon excitation of GaAs. We determined the electron polarization for three GaAs sample thicknesses using a compact retarding-field micro-Mott polarimeter. Two-photon absorption with 1560 nm light was verified by noting that quantum efficiency varied linearly with laser intensity, which was adjusted by various means. For each photocathode the degree of spin polarization of the photoemitted beam was less than 50%, with the same sign as that from our one-photon measurements, contradicting both the prediction and photoluminescence measurements of Matsuyama et al. [12,13]. Polarization via two-photon absorption was the highest from the thin photocathode samples and comparable to that obtained via one-photon 778 nm absorption ($\sim 43\%$).

2. Theoretical considerations

Although spin-parity selection rules would bar a two-photon transition for a free atom, Bhat et al. [14] show that dipole-forbidden transitions are allowed in GaAs near the Γ point. To summarize the findings of Bhat the structure of a GaAs crystal violates the spherical symmetry of single-atom fields, which leads to the non-conservation of angular momentum for $\vec{k} \neq 0$. The perturbation of this spherical symmetry is very small for electrons near the center of the Brillouin zone, which is why the angular momentum is still an approximate quantum number for electron transitions induced by one-photon absorption in a direct band-gap transition. For two-photon absorption, the picture is more complicated, as spherical symmetry forbids such transitions at the center of the Γ point. However, because of the crystal lattice perturbation, there can be weak two-photon absorption in this region. In this interaction, there is a lack of angular momentum conservation between the incident photon and excited electron, which precludes electron polarization for two-photon absorption from being above 50%. Indeed, Bhat et al. [14] predict a polarization just above the band-gap threshold of $\sim +49\%$ at 1560 nm, while the work in Ref. [12] predicts complete polarization of the opposite sign. Our experiment was performed to differentiate between the two predictions.

3. Experimental setup

Our apparatus consisted of a low-voltage polarized electron source chamber for installing and activating photocathodes, a beam transport section, and a micro-Mott retarding-field

polarimeter (Fig. 2). Unstrained bulk GaAs was mounted on a long stalk that could be lowered into the source chamber. The GaAs was then activated, and reactivated as needed, by heating to $\sim 550^\circ\text{C}$ to clean the surface and then by applying Cs and NF_3 to create a surface with negative electron affinity [16]. Three different wafers of unstrained GaAs were used. One sample, known as the “thick” sample ($625\ \mu\text{m}$), was epi-ready unstrained bulk GaAs, with a (1 0 0) surface, p-doped with a Zn density of $\sim 5 \times 10^{18}/\text{cm}^{-3}$. The “thin” samples (0.18 and $0.32\ \mu\text{m}$) were grown via MOCVD with p-doping of Zn (density $\sim 4 \times 10^{18}/\text{cm}^{-3}$) on thick GaAs substrates, with an intervening barrier layer of p- $\text{Al}_{0.3}\text{Ga}_{0.7}\text{As}$ that was $\sim 0.9\ \mu\text{m}$ thick. The band gap of this barrier layer is much larger than that of GaAs, which ensured that no photoemission originated in the barrier layer from either 780 nm or 1560 nm light and also that any electrons excited in the substrate material did not reach the photocathode surface. For all GaAs samples, the photocathode was biased at $-268\ \text{V}$ using batteries and the emitted electron beam was delivered to the micro-Mott polarimeter using a 90° electrostatic deflector and electrostatic steering lenses [17,18]. The beam transport system and the micro-Mott polarimeter are described more thoroughly in another publication [19].

Two laser wavelengths were used: i.e. 778 and 1560 nm for one- and two-photon absorption, respectively. Optical systems for each wavelength could be quickly and reproducibly moved in and out of position beneath the vacuum chamber. When the 1560 nm laser system was in place (Fig. 3), long-pass optical filters (two at 1350 nm and one at 850 nm) were inserted into the laser path to

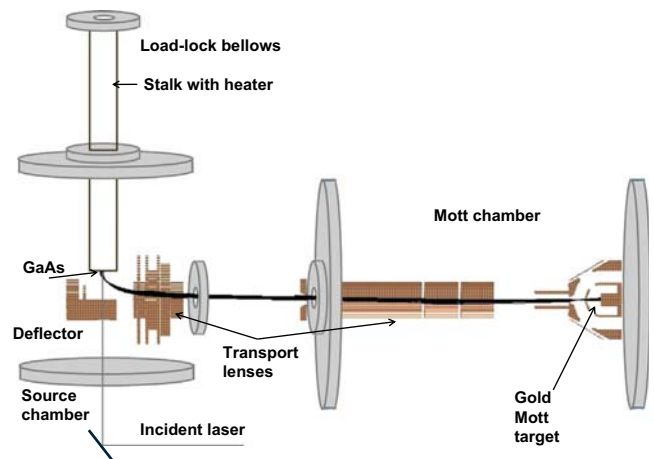


Fig. 2. Schematic of the experimental apparatus, with source chamber, transport, and Mott chamber sections. The black lines directed through the lenses represent electron trajectories simulated by SIMION.

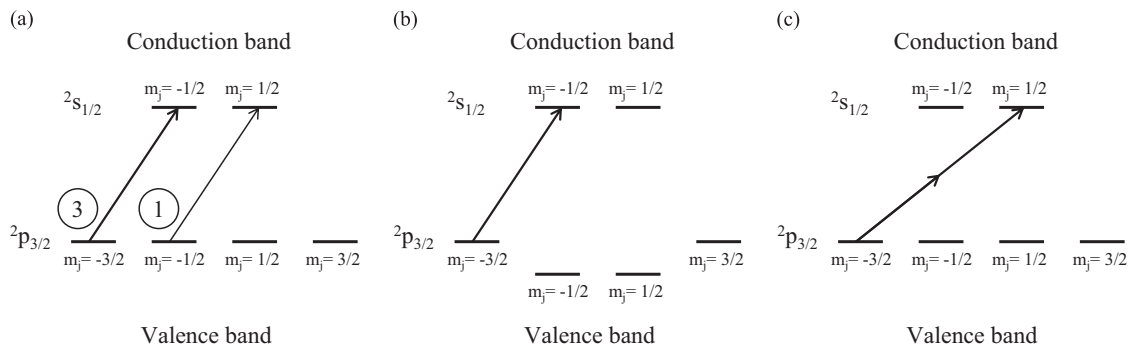


Fig. 1. Various means to populate the conduction band of GaAs with circularly-polarized light: a) one-photon excitation of unstrained GaAs, b) one-photon excitation of strained GaAs, and c) two-photon excitation of unstrained GaAs with photons having energy equal to half that of the bandgap. The circled values in (a) indicate relative transition probabilities for unstrained GaAs. The maximum theoretical polarization is 50% from unstrained bulk GaAs via one-photon absorption, 100% from strained GaAs via one-photon excitation, and -100% from unstrained GaAs via two-photon excitation, at least in the simple selection-rule picture of Ref. [12].

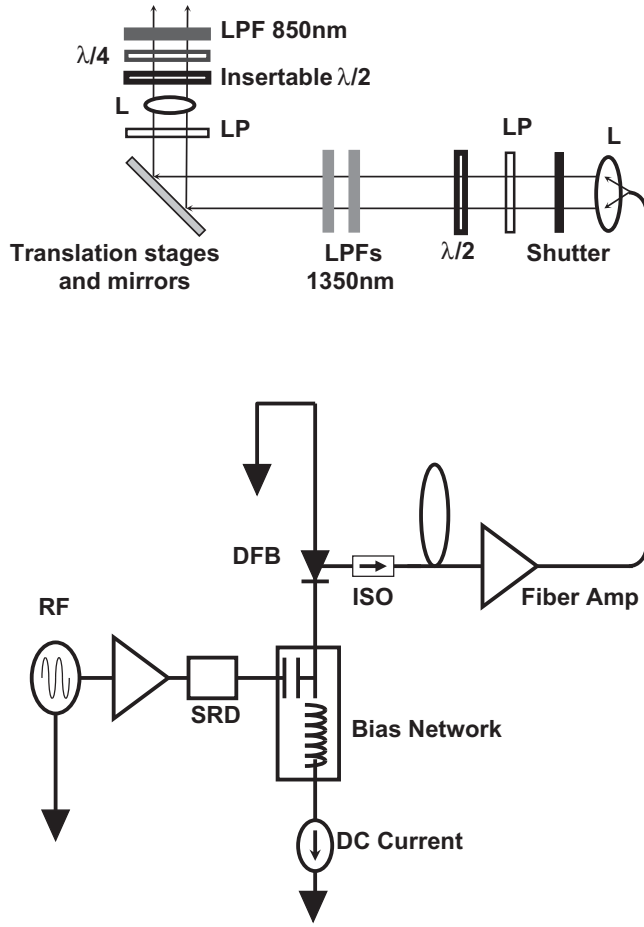


Fig. 3. Schematic of the 1560 nm light source used to generate a two-photon photo-emitted electron beam from un-strained bulk GaAs showing DFB, distributed feedback Bragg reflector diode laser; ISO, fiber isolator; SRD, step recovery diode; L, lens; LP, linear polarizer; $\lambda/2$ and $\lambda/4$, half-wave and quarter-wave plates; LPF, long pass filter.

ensure that no light below 850 nm could enter the vacuum apparatus and illuminate the photocathode. A mirror system mounted on dual translation stages directed the laser beam vertically into the source chamber and provided a means to map the quantum efficiency of the photocathode (see below).

The 778 nm light source was a simple low-power diode laser operating either in DC or RF pulsed-mode via gain-switching at repetition rates from 250 to 1000 MHz. The quantum efficiency (QE) at 778 nm for one-photon absorption, QE_{ω_1} , should be independent of incident laser intensity, and thus independent of average power, peak power, or laser spot size.

The 1560 nm laser was a gain-switched fiber-coupled diode “seed” laser and fiber-amplifier (Fig. 3) that produced up to 5 W average power at repetition rates from 250 to 2000 MHz, with optical pulse widths of ~ 40 – 60 ps, depending on the rate [20]. By using short-pulse light, high peak power was obtained to enhance the two-photon absorption process. For two-photon absorption, the QE at 1560 nm, $QE_{2\omega}$, should vary proportionally with laser intensity, as the light absorption is quadratic with intensity. In this experiment, there were three “knobs” used to vary the laser intensity at the photocathode: the average power of the light, the spot size of the laser on the photocathode, and the pulse repetition rate (while keeping pulse widths similar and average power constant). These parameters affect the average and peak intensities at the photocathode:

$$I_{avg} = P_{avg}/A \quad (1)$$

and

$$I_{peak} = \frac{I_{avg}}{\mathfrak{D}} = \frac{P_{avg}}{A\mathfrak{D}} = \frac{P_{avg}}{Atf}, \quad (2)$$

where P_{avg} is the average power of the laser, \mathfrak{D} is the duty factor (the product of the optical pulse width t and the laser pulse repetition rate f), and A is the spot size of the laser on the photocathode.

Different laser spot sizes were obtained by using lenses of different focal lengths. A 30 cm focal-length lens in the optical train below the vacuum window was used to produce a beam focal waist of $270 \mu\text{m}$ FWHM at the photocathode; longer focal-length lenses placed at the same location produced larger beam waists, up to $1200 \mu\text{m}$ FWHM. Because changing lenses in the optical system could potentially vary the beam trajectory, QE scans (see below) were performed after each change of lens or light source in order to facilitate direct comparisons of measurements.

The RF-pulsed nature of the laser systems provided a means to easily vary the peak intensity of the light at the photocathode. Because the fiber amplifier provided the same average output power for each repetition rate, the peak intensity of the laser system could be varied by changing the pulse repetition rate, with the highest intensity obtained at lower pulse repetition rates.

Several steps were taken to ensure that the surface states of the photocathode were the same for the pairs of measurements comparing the one- and two-photon processes. Each set of QE and polarization data was taken during the same photocathode activation. However, because the Cs deposition at the photocathode was non-uniform, the QE of the GaAs wafer varied over its surface. The QE was measured using a picoammeter in series with the biased cathode and ground. Using the x - y translation stages underneath the vacuum window, “QE scans” were performed by measuring the QE across the cathode. Because of the simple design of the electrostatic lenses used to bend the electron beam 90° from the photocathode to the Mott target, the amount of beam transmission from the photocathode to the polarimeter was not constant across the photocathode. By connecting another picoammeter to the Mott target, biased at $\sim +300$ V while performing a QE scan, a map of photocurrent transmission from the cathode to the polarimeter could also be made. The highest transmission, corresponding to about 20% of the photoemitted beam striking the polarimeter target, occurred for emission from a specific location of the GaAs photocathode about 2 mm in diameter, whereas the entire activated photocathode was ~ 12 mm in diameter. The areas of highest transmission and that of highest QE were located roughly 6 mm apart. Unless otherwise noted, QE data is presented at the location of highest QE of the photocathode, and polarization data were always taken at the highest transmission location of the photocathode.

4. Results and discussion

4.1. One- and two-photon quantum efficiency

The $625 \mu\text{m}$ thick unstrained bulk GaAs was first evaluated using 778 nm light. As expected, QE_{ω_1} remained fairly constant vs. input power and pulse repetition rates (Fig. 4a). Because of the range of powers used, the abscissa in Fig. 4a is plotted logarithmically. There was a slight decrease in QE_{ω_1} as the laser power increased for a given repetition rate, which can be attributed to the surface charge limit effect due to the relatively large peak current (up to $\sim 800 \mu\text{A}$) that was extracted [21]. In addition, a decrease in QE_{ω_1} observed with increasing intensity (lower repetition rates) at a given average power can be explained by the space charge effects of the shorter electron bunches [21].

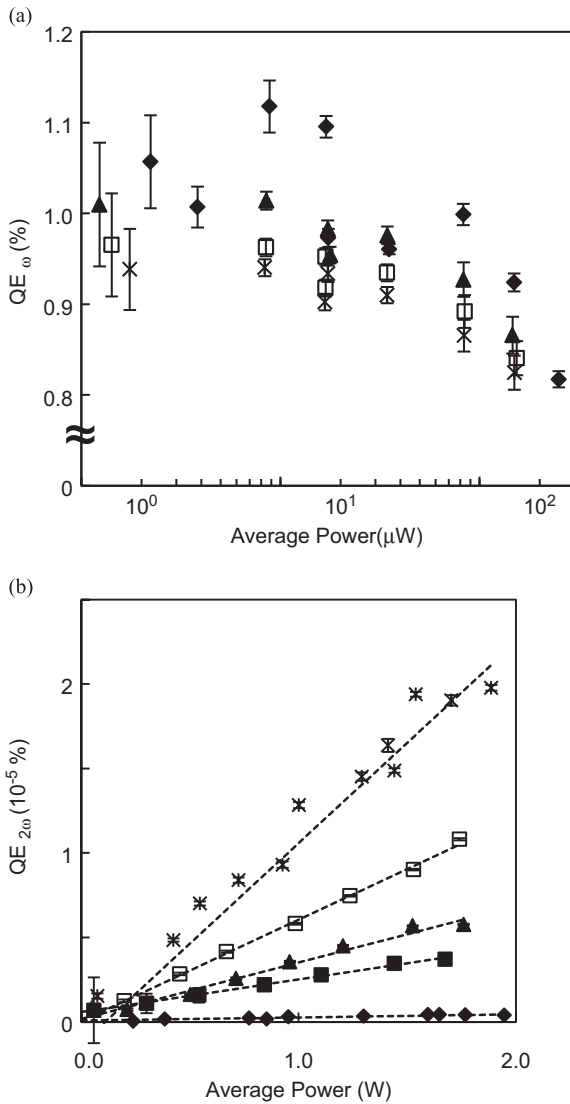


Fig. 4. a) Representative QE_{ω} vs. input power at 778 nm, for the laser pulse repetition rates given below, and b) representative $QE_{2\omega}$ at 1560 nm. Dashed lines represent linear fits to the data for a given repetition rate. The repetition rate legend is the same for both plots: DC (\blacklozenge), 2000 MHz (\blacksquare), 1000 MHz (\blacktriangle), 500 MHz (\square), and 250 MHz (\ast). 2000 MHz data is not included in (a).

The $QE_{2\omega}$ behavior at 1560 nm (Fig. 4b) was qualitatively different from the behavior of $QE_{2\omega}$ at 778 nm. Indicative of a two-photon-absorption process, higher light intensity produced higher $QE_{2\omega}$, which increased linearly with power and intensity. Using the 1560 nm source, a maximum photocurrent of ~ 5 nA was measured at 250 MHz and 1.9 W. The demonstrated linear increase with power for each individual repetition rate provides clear evidence for a two-photon photoemission process.

Next, using a pulse repetition rate of 250 MHz, the laser intensity was varied by changing the size of the laser spot at the photocathode, with the QE results shown in Fig. 5. As noted above, the photocathode activation was not uniform across the surface, causing the location of maximum QE to not be coincident with the location of maximum beam transmission to the polarimeter. Scans of QE were performed, with comparative measurements at both wavelengths always being performed at the same photocathode location. The measurements in Fig. 5 show results from both the maximum QE (\blacksquare) and the QE at the maximum transmission locations (\blacktriangle). At 778 nm (Fig. 5a), the QE_{ω} was nearly constant vs. peak intensity, with any deviation attributable to averaging

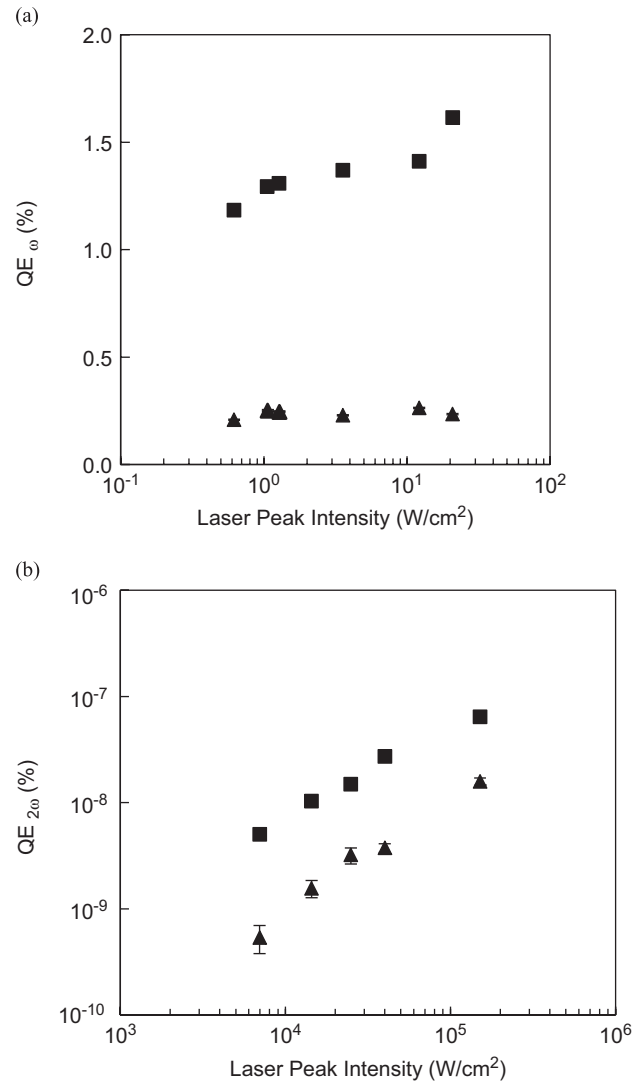


Fig. 5. QE vs. peak intensity of the laser beam caused by changing the laser spot size at the cathode. The QE across the photocathode was not uniform: maximum QE (\blacksquare) and maximum transmission location QE (\blacktriangle) at the photocathode location for maximum transmission to the polarimeter (see the text). a) QE_{ω} at 778 nm. b) $QE_{2\omega}$ at 1560 nm. Data were obtained using a laser repetition rate of 250 MHz.

over the non-uniform surface with different laser spot sizes. Because the maximum QE was found at the very edge of the photocathode, sampling the location with a smaller, more intense laser spot had the effect of slightly raising the measured QE. The smaller laser spots were fully incident on the photocathode, while the larger spots also overlapped an electrostatic bend electrode. The behavior at 1560 nm was quite different from that at 778 nm, as $QE_{2\omega}$ increased linearly with laser peak intensity (Fig. 5b), as expected. Here again, the two-photon process is shown qualitatively to be the dominant mechanism in the absorption of 1560 nm light in GaAs.

4.2. Electron polarization from thick (625 μ m) unstrained GaAs

The polarization asymmetry of the electron beams generated with one- and two-photon excitation was measured using the micro-Mott polarimeter, in the manner described in Ref. [19] with the target biased at 20 kV and with a maximum electron energy loss in the target $\Delta E=0$. The quantity $\Delta E=0$ is the greatest energy loss an electron scattered by the Mott target can suffer and still be detected. The electron polarization was determined using the

Table 1

Photoemitted electron polarization taken for one- and two-photon absorption for three different samples of GaAs.

Active thickness	Photoelectron polarization (%)	
	One-photon (778 nm)	Two-photon (1560 nm)
0.18 μm	42.6 \pm 1.0	40.3 \pm 1.0
0.32 μm	44.0 \pm 1.1	36.0 \pm 0.9
Bulk material	33.4 \pm 0.8	16.8 \pm 0.4

equation $P_e = A_{meas}/S_{eff}$, where A_{meas} is the measured Mott polarimeter asymmetry, and S_{eff} is the effective Sherman function, which was evaluated previously and found to be 0.201 ± 0.005 [19]. Repeated measurements indicated that the polarization at both 1560 nm and 778 nm was stable with regard to extracted photocurrent, with a polarization at 778 nm of $33.4 \pm 0.8\%$, which is typical of bulk GaAs. At 1560 nm, the measured polarization was $16.8 \pm 0.4\%$, which is significantly lower than any prediction, even when accounting for depolarization effects similar in magnitude to those for photoelectrons created at 778 nm. Importantly, the sign of the beam polarization obtained via two-photon absorption was the same as that obtained via one-photon absorption.

4.3. Electron polarization from thin unstrained GaAs

One reason for the lower-than-expected value of polarization associated with two-photon emission is that 1560 nm light has a very large absorption depth in GaAs. The long absorption depth leads to long exit paths of the electrons, and hence more depolarization. It was not clear from the bulk sample measurements if the lower-than-expected two-photon polarization was due to the long electron diffusion paths to the cathode surface or to an unexpectedly low value of initial two-photon polarization, in contradiction to Ref. [14]. The photoelectron polarization was thus measured using samples with thicknesses significantly less than the expected electron spin-depolarization length l_{sp} [22]. GaAs samples with active thickness of 0.18 μm or 0.32 μm were analyzed using the same settings of the micro-Mott polarimeter as those of the bulk sample. For the thinnest GaAs sample, the polarizations with one- and two-photon absorption were only slightly different, $\sim 43\%$ vs. 40% , respectively, as seen in Table 1. While theoretically one-photon absorption should give 50% polarization, there are many effects which reduce the polarization, even with thin active layers, and the measured $\sim 43\%$ polarization at 778 nm is typical of thin unstrained GaAs [23]. The convergence of the two-photon polarization to that of the one-photon polarization with decreasing sample thickness indicates an initial two-photon polarization close to 50%, as proposed by Bhat et al. [14]. As such, two-photon absorption appears to be incapable of producing an electron beam with polarization greater than 50%.

5. Conclusion

Two-photon photoemission was used to generate electron beams from unstrained GaAs photocathodes of varying thickness:

625 μm , 0.32 μm and 0.18 μm . Polarization via two-photon absorption from the thickest sample was approximately half of that obtained via one photon absorption, and had the same sign. For the thinner samples, polarizations via two and one-photon absorption were comparable, $\sim 40\%$ vs. 43% , respectively, with the degree of spin polarization of the photoemitted beam always less than 50%. These results indicate that the two-photon transition depicted in Fig. 1c does not occur with significant probability. Though the two-photon polarization approaches the one-photon polarization, the figure of merit (defined as polarization squared, multiplied by beam current) for a two-photon GaAs polarized source is many orders of magnitude lower than those of existing one-photon sources, because $QE_{2\omega}$ is many orders of magnitude lower than QE_{ω} of even strained-superlattice GaAs photocathodes. As such, the current implementation using two photons at half the band-gap in a polarized GaAs source is untenable, which leaves strained GaAs and its variants as the only available highly polarized photoemission source at this time.

Acknowledgments

We thank Steve Covert, Jim Clark, Marcy Stutzman and Phil Adderley for assistance with the apparatus, and acknowledge useful discussions with Leonid Gerchikov of St. Petersburg State Polytechnic University, Russia, regarding theoretical models of two-photon photoemission and polarization. This work was supported by Jefferson Science Associates, LLC under U.S. DOE Contract no. DE-AC05-06OR23177 and by NSF Grants PHY-0821385 and PHY-1206067 (TJG).

References

- [1] H. Montgomery, J. Phys.: Conf. Ser. 299 (2011) 011001.
- [2] C.Y. Prescott, et al., Phys. Lett. B 77 (1978) 347–352.
- [3] D.T. Pierce, F. Meier, Phys. Rev. B 13 (1976) 5484–5500.
- [4] J. Kessler, Polarized Electrons, 2nd edition, Springer, New York, 1985.
- [5] T. Maruyama, et al., Phys. Rev. Lett. 66 (1991) 2376.
- [6] T. Nakanishi, et al., Phys. Lett. A 158 (1991) 345–349.
- [7] T. Maruyama, et al., Phys. Rev. B 46 (1992) 4261.
- [8] T. Nakanishi, et al., AIP Conf. Proc. 421 (1998) 300–310.
- [9] J. Jian, et al., Appl. Phys. Lett. 85 (2004) 2640.
- [10] H. Aoyagi, et al., Phys. Lett. A 167 (1992) 415.
- [11] A. Yariv, Optical Electronics, Holt, Rinehart and Winston, New York, 1985.
- [12] T. Matsuyama, et al., in: Proceedings of the 4th Pacific Rim Conference on Lasers and Electro-Optics, 2001, pp. 164–165.
- [13] T. Matsuyama, et al., Jpn. J. Appl. Phys. 40 (2001) 555–557.
- [14] R.D.R. Bhat, et al., Phys. Rev. B 71 (2005) 035209.
- [15] M.I. Miah, J. Phys. Chem. B 113 (2009) 6800–6802.
- [16] C.K. Sinclair, et al., Phys. Rev. Spec. Top.: Accel. Beams 10 (2007) 023501.
- [17] H.M. Al-Khateeb, et al., Rev. Sci. Instrum. 70 (1999) 3882.
- [18] T.G. Anderson, et al., Rev. Sci. Instrum. 72 (2001) 2923.
- [19] J.L. McCarter, et al., Nucl. Instrum. Methods A 618 (2010) 30–36.
- [20] J. Hansknecht, M. Poelker, Phys. Rev. Spec. Top.: Accel. Beams 9 (2006) 063501.
- [21] M. Woods, et al., J. Appl. Phys. 73 (1993) 8531–8535.
- [22] R.I. Dzhiyev, et al., Phys. Solid State 45 (2003) 2255.
- [23] P. J. Saez, (Ph.D. thesis), Stanford University, 1997.